2011

Horizontal Propagation Deep Turbulence Testbed

Corley, M.S.; Santiago, F.; T. Martinez; Agrawal, B.N.

Horizontal propagation deep turbulence test bed

Melissa Corley[1], Freddie Santiago[2], Ty Martinez[2], Brij N. Agrawal[1]

[1]*Naval Postgraduate School, Monterey, California*

[2] *Naval Research Laboratory, Remote Sensing Division, Code 7216, Washington, DC*

[*]*Corresponding author: fsantia@sandia.gov*

Abstract

The Navy is interested in horizontal laser propagation studies in a maritime environment, near the ocean surface, for applications including imaging and high-energy laser propagation. The Naval Postgraduate School (NPS) in Monterey, California, and the Naval Research Laboratory (NRL) Wavefront Sensing and Control Division in Albuquerque, New Mexico, are collaborating in the development of a horizontal propagation testbed with adaptive optics for correction and simulation of atmospheric deep turbulence conditions. Atmospheric turbulence near the ocean surface is mostly dominated by scintillation, or intensity fluctuations, which degrade beam quality as propagation distance increases. While statistical data has been collected and analyzed for decades on the vertical turbulence profile, horizontal, deep turbulence data collection has begun only relatively recently. No theoretical model currently exists to describe horizontal turbulence that parallels the familiar Kolmogorov statistical model used in vertical AO applications, and investigations are underway to develop such models.

The main purpose of the NPS testbed is to develop an adaptive optics system which is capable of simulating scintillation effects. Since it is known that branch points and scintillation are characteristic of the deep turbulence problem, the testbed developed for this research is used to simulate the effects of intensity fluctuations and intensity dropouts on the Shack-Hartmann WFS. This is accomplished by applying atmosphere on two separate Spatial Light Modulators (SLMs), both individually and simultaneously, and extending the beam path between them to observe the atmospheric disturbances produced. These SLMs allow the implementation of various atmospheric turbulence realizations, while the use of two in combination allows the simulation of a thick aberrator to more closely approximate horizontal turbulence behavior. The short path length allows a propagation distance of approximately 2 meters between the SLMs, while the long path allows approximately 22 meters.

Images of Shack Hartmann wavefront sensor spots show intensity fluctuations similar to those observed in actual maritime experiments. These fluctuations are used to quantify intensity dropouts in both the short and long paths. Intensity dropouts due to the atmospheric distortions in the short path represent 0.5–1% of total sensor subapertures, while the long path distortions introduce 5–10% intensity dropouts. Further analysis is performed on the images from the long path to estimate the atmospheric structure constant, C_n^2, from scintillation calculations, resulting

in a C_n^2 value of approximately 9.99x10^{-11} m$^{-2/3}$ for the short path and 4.26x10^{-11} m$^{-2/3}$ for the long path.

This paper presents a description of the optical testbed setup, the details of horizontal turbulence simulation, and the results of the scintillation calculations resulting from data collected in the laboratory. The success of this experiment lays an important foundation for simulating maritime-like horizontal atmosphere in the laboratory for beam control in HEL ship systems.

1.0 Introduction

While statistical data has been collected and analyzed for decades on the vertical turbulence profile, horizontal, deep turbulence data collection has begun only relatively recently. No theoretical model currently exists to describe horizontal turbulence that parallels the familiar Kolmogorov statistical model used in vertical AO applications, and investigations are underway to develop such models. During the past decade, specifically due to Navy interest, several research projects have begun. For example, experiments have been performed by SPAWAR in San Diego over a 7.07km path at Zuniga Shoal to gather data on predicting the atmospheric structure constant, C_n^2, which is integral to the development of a theoretical model of maritime turbulence (Hammel et al., 2007). This work also used the Navy Surface Layer Optical Turbulence (NSLOT) model developed at NPS, which depends primarily on local air and sea temperature measurements. Additionally, the Naval Research Laboratory (NRL) and University of Puerto Rico at Mayagüez have collected horizontal propagation data over water at the Island of Magueyes in Puerto Rico (Santiago, et al, 2005), the University of Florida has taken measurements over maritime paths to study C_n^2 (Vetelino, et al., 2006), and Michigan Tech has begun horizontal path experiments over land and water to develop statistics of the atmospheric coherence length or Fried parameter, r_0 (Sergeyev & Roggemann, 2010).

NPS and NRL's main focus is to develop a laboratory testbed in which conditions similar to the deep turbulence regime, particularly scintillation conditions, can be replicated. Simulating this regime allows testing of new adaptive optics techniques, control algorithms, and new horizontal atmospheric turbulence models resulting from gathered data. Scintillation effects in low astronomical elevation angles and horizontal propagation are one of the main challenges for AO systems. In addition, branch points, or discontinuities in the optical phase, present a challenge for wavefront sensors in AO systems (Fried, 1992; Fried, 1998; Sanchez & Oesch, 2009). Branch points are associated with $\pm 2\pi$ jumps or singularities in the phase and occur when the amplitude or intensity in the beam drops to zero. These singularities decrease the effectiveness of many classical wavefront sensors which provide phase and wavefront slope information to the corrector. While the wavefront sensor is designed to detect phase aberrations that can be reconstructed and corrected for, the introduction of phase discontinuities and amplitude variations resulting from scintillation and branch points can corrupt the pure phase measurements, leading to inaccurate wavefront information. Humidity and temperature fluctuations, aerosols, and wave motion are other marine characteristics that affect turbulence.

The research presented here focuses on the development of a laboratory testbed for deep turbulence conditions, on which a thick aberrator with scintillation effects and dropouts was generated, advanced AO beam control algorithms were tested, a simple dropout detection

algorithm was implemented, and scintillation analysis was performed. This paper does not present the beam control algorithms themselves, but rather focuses on the experimental setup, the horizontal turbulence simulation, and the scintillation analysis.

2.0 Laboratory Test bed

Figure 1 shows the adaptive optics testbed with primary components labeled, and Figure 2 shows a schematic of the AO system with four available beam paths.

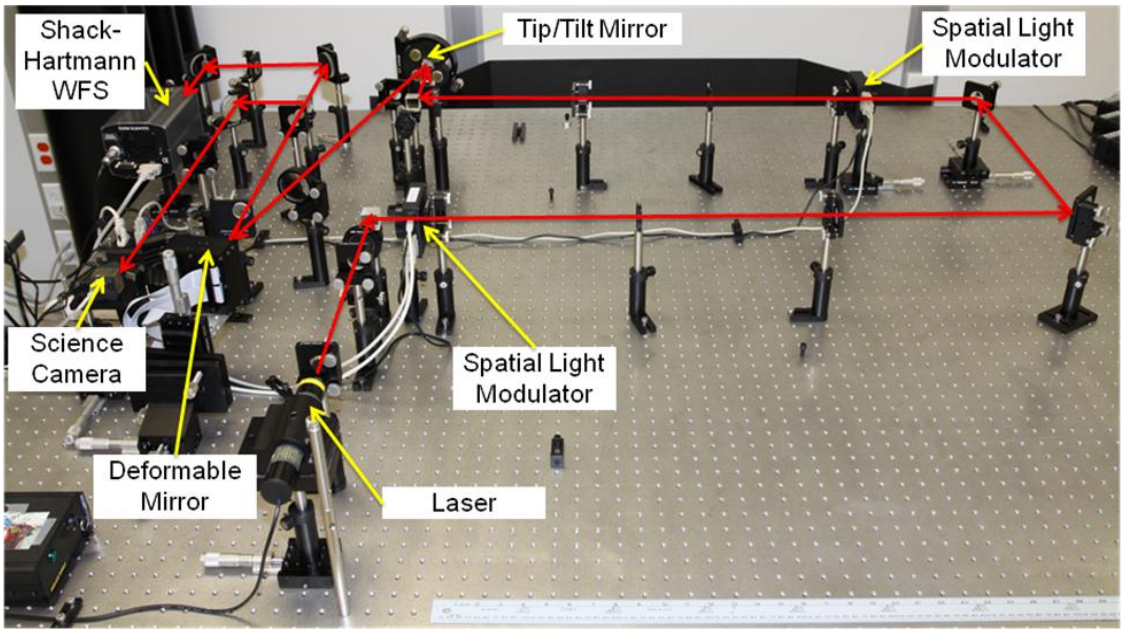

Figure 1 - Laboratory testbed showing primary components

Initial control algorithm testing was performed using this initial configuration, which will be referred to as the short path. The deep turbulence scenario was created by extending the beam path in a configuration referred to as the long path. The setup can be changed quickly and easily to support either the short or long path by using a translation stage to move only two mirrors. These mirrors break and return the beam to its original path, and can be moved in or out of the original path as desired. Figure 3 shows the updated configuration, and Figure 4 shows a schematic with the long path extension in blue. The short path length allows a propagation distance of approximately 2 meters between the SLMs, while the long path allows approximately 22 meters.

The Naval Research Laboratory (NRL) has developed software to apply atmospheric aberrations on two SLMs using a Matlab graphical user interface (GUI). This software is based on traditional Kolmogorov statistics for astronomical applications, but as new models more suitable for maritime environment are developed it can be modify to accommodate the changes.

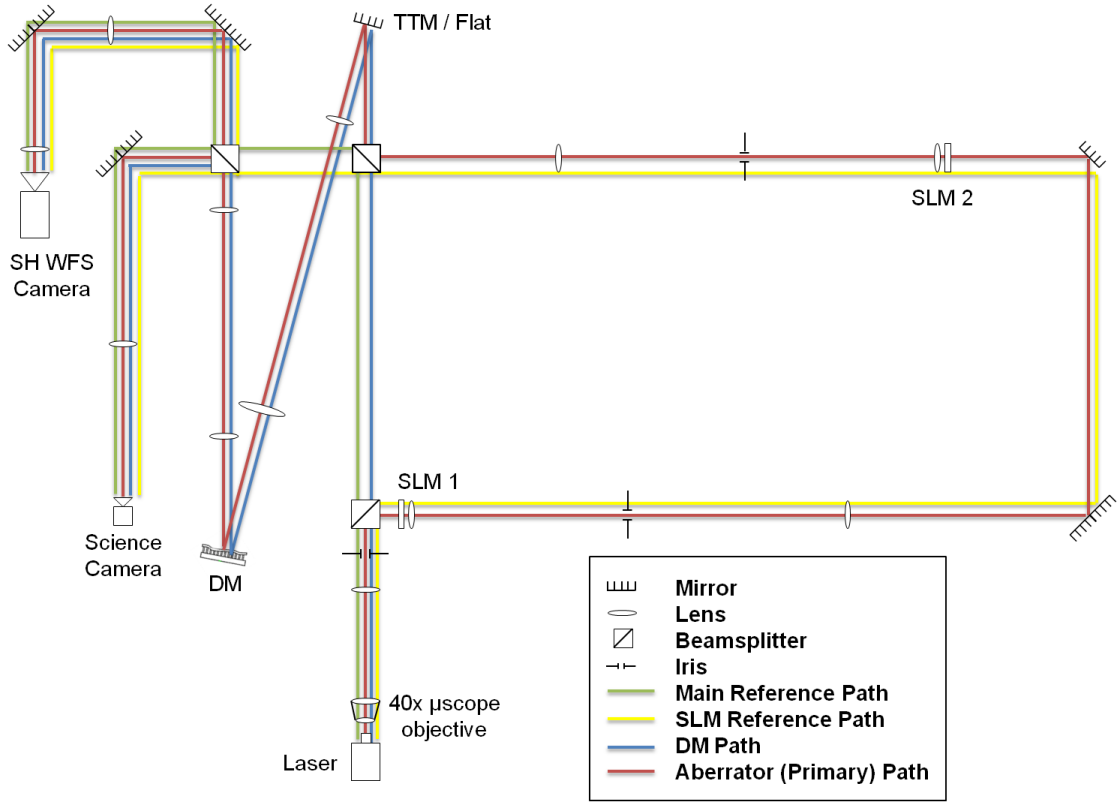

Figure 2 – Schematic of laboratory system in short path

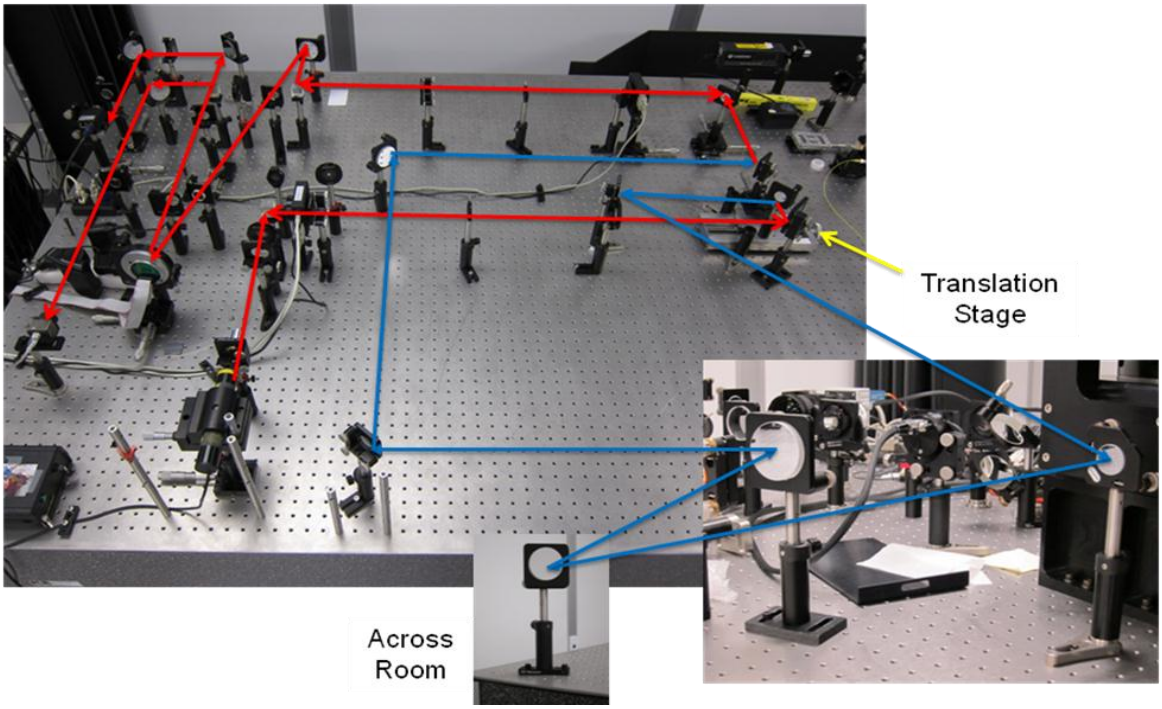

Figure 3 – Modified testbed showing long path extension in blue

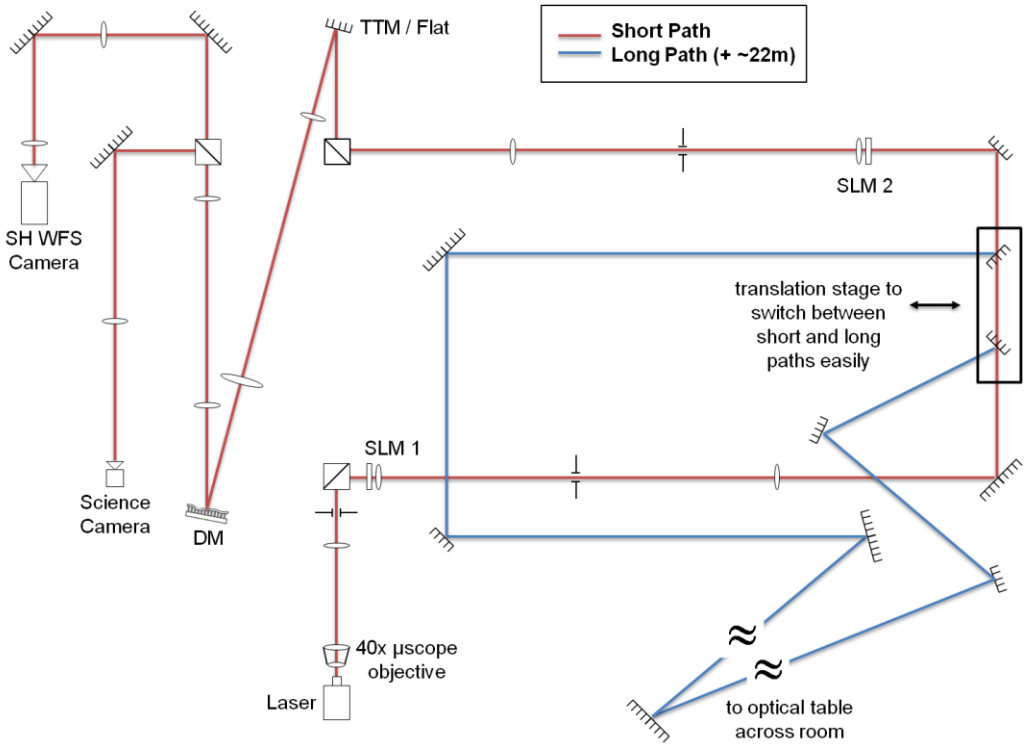

Figure 4 – Schematic showing beam path extension and translation stage location

Figure 5 shows a conceptual diagram of what happens to the beam in each of the configurations available. In the short path, the image of aberrations applied at SLM 2 will be sensed accurately at the wavefront sensor since they are in conjugate planes. When the atmosphere is applied at SLM 1, some additional propagation distance will be included. However, it is expected that the propagation distance is not long enough to cause deep turbulence effects, and that the wavefront sensor reconstruction of the phase aberrations will still be fairly comparable to those of SLM 2. If the error is similar to that of SLM 2, it can be concluded that some uncertainty in determining the location of the aberration plane in a real scenario can be accepted.

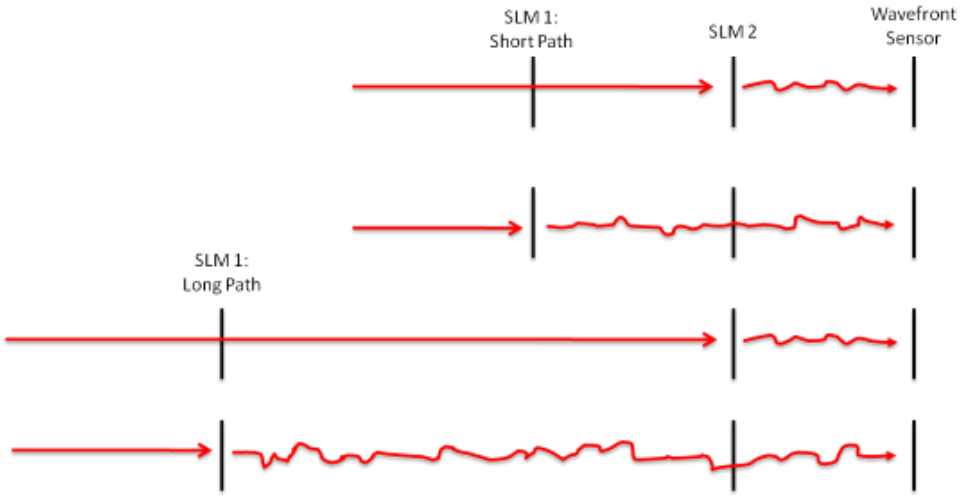

Figure 5 – Visualization of beam path configurations

In the long path shown in Figure 5, it is expected that the image of aberrations applied at SLM 2 will include some contribution from atmospheric effects in the room, leading to higher variations in the wavefront slope error. However, since the SLM atmospheric phase profile is still applied in the system pupil plane, the phase aberrations should still be sensed fairly accurately at the wavefront sensor. On the other hand, when phase aberrations are applied at SLM 1 in the long path, upstream of the beam path extension, they propagate through a much longer distance before reaching the wavefront sensor. It is at this point that intensity fluctuations and dropouts are expected to contribute significantly to the disturbance profile sensed at the wavefront sensor.

3.0 Deep turbulence test bed results

Since it is known that branch points and scintillation are characteristic of the deep turbulence problem, the testbed developed for this research is used to simulate the effects of intensity fluctuations and intensity dropouts on the Shack-Hartmann WFS. Before applying atmosphere to the SLMs in the long path, wavefront sensor images of the SLM reference beam were recorded in the long path to determine whether the path extension through ambient atmosphere alone produces noticeable changes in the intensity profile of the laser beam. The wavefront sensor images show that there is indeed a significant difference in the behavior of WFS lenslet spots on the camera. The long path beam visibly fluctuates across the lenslets more than the short path beam. While the fluctuations are more apparent in video, the images show every other frame of 12 frames for each path. The overall intensity level is lower in the long path due to diffraction effects and the increased number of mirror reflections. The fluctuations rather than the intensity represent the difference between the image sequences. The simplest variation to see is the changing intensity of brighter hot spots in some of the central lenslets throughout the long path frames.

With intensity fluctuations demonstrated in the long path due to ambient atmospheric conditions only, it is expected that propagating atmosphere from SLM 1 through the long path will yield the desired intensity fluctuation and dropout behavior for simulating the effects of deep turbulence. While the long path effects are expected to slightly increase the variation of wavefront sensor error in the presence of atmosphere applied on SLM 2, it is still expected that the wavefront sensor will be able to detect the phase aberrations fairly well, since the stronger applied atmosphere will not have propagated the long distance.

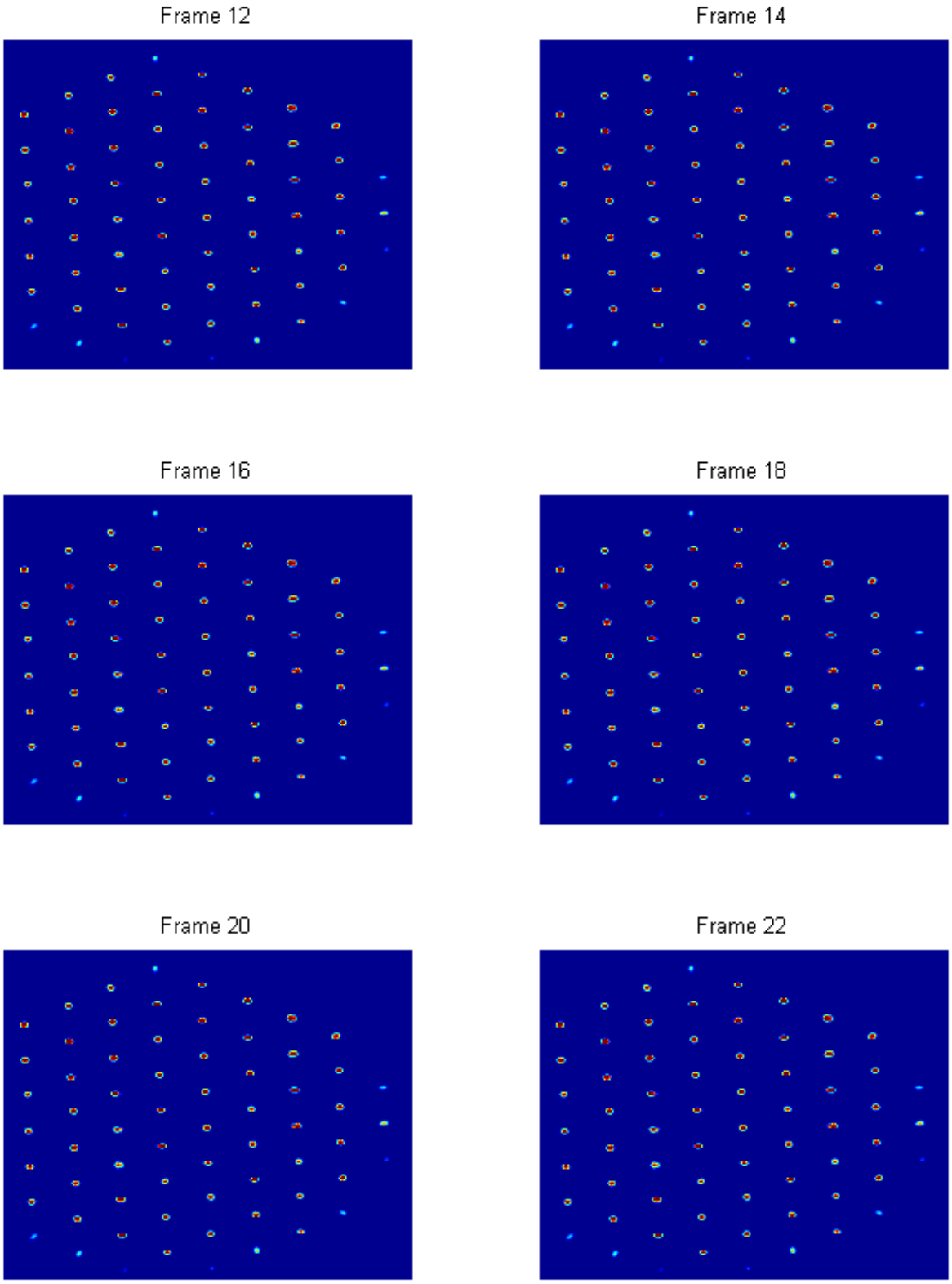

Figure 6 – WFS images in short path, no SLM aberrations

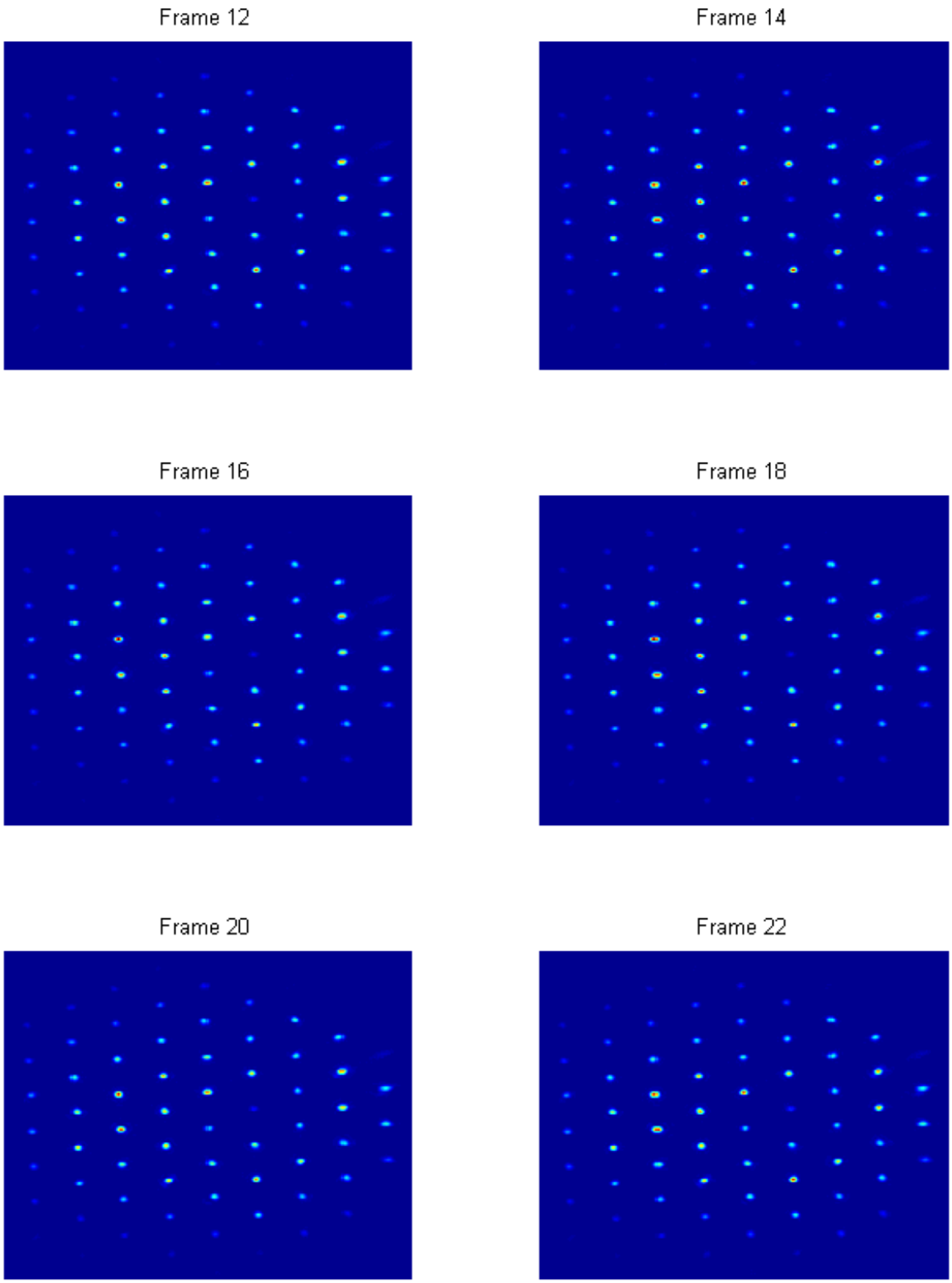

Figure 7 – WFS images in long path, no SLM aberrations

3.1 Intensity dropouts

Once the effects of intensity fluctuations and dropouts in the long path were observed visually, a rudimentary detection method was developed in software and implemented in the WFS centroiding algorithm. Using the 8-bit Basler camera with low noise, the Shack-Hartmann WFS subapertures sense only the lenslet spots themselves above a zero threshold. If a spot drops out completely, the subaperture contains only zero-valued pixels. This work found that it is possible to use this information both as an indication of the presence of an intensity dropout, and to assign a placeholder value for the missing centroid.

The centroiding algorithm, which determines the lenslet spot offsets from the reference centroids, is modified to detect dropouts as follows. If a WFS subaperture contains only zero-valued pixels, the algorithm returns an indication of an intensity dropout, a (1). If there is no dropout, the algorithm returns a (0). In the former case in the absence of a centroid reading, the centroid is artificially set to return the centroid position as the bottom right corner of the subaperture. This is done to induce high slope error, since the reference centroids from which the offsets are determined are close to the center of the subaperture. While this method of artificially assigning a centroid location is understood to produce some inaccurate error results, it is implemented for simplicity and the visualization of error trends in the disturbance profiles. Once it has been determined that dropouts occur, and to what extent they occur in the short and long paths, more appropriate methods of estimating centroid locations or trajectories in case of a dropout can be developed. To demonstrate the outcome of this simple detection method, the beam is blocked manually by an index card. Figure 6 shows the long path reference image overlaid with reference grid locations. The subapertures containing intensity dropouts during partial obscuration of the beam are marked by blue stars. The dropouts are detected as expected.

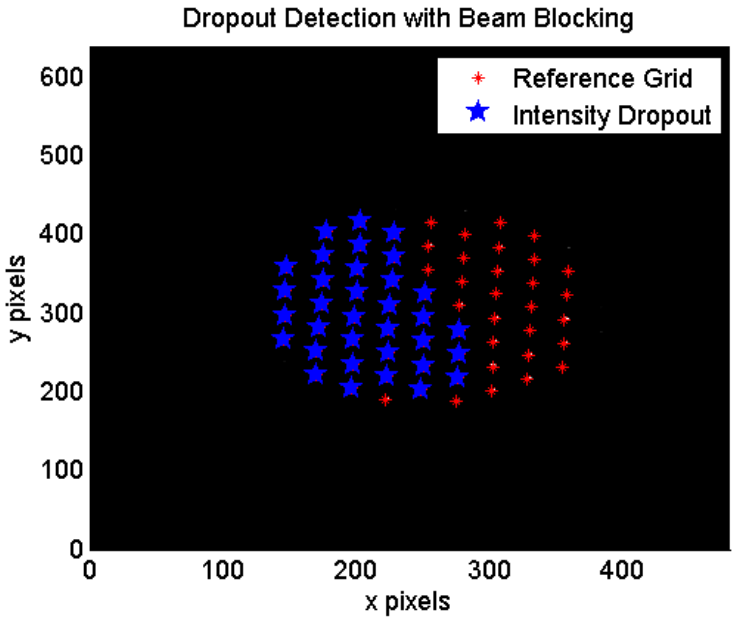

Figure 8 – Intensity dropouts caused by manually blocking laser beam

3.2 Dropout Detection with Atmosphere

With dropout detection in place, atmospheric data is collected in 20-second intervals in both the short and long paths to determine the number of intensity dropouts in each case and the trends followed by the disturbance data. Four rates of the same atmospheric realization are recorded. The atmospheric realization is run at 1 Hz, 3 Hz, 5 Hz, and 7.5 Hz on SLM 2 alone, SLM 1 alone, and on both SLMs together. Table 5 shows the number of dropouts in each case, and the percentage of total possible dropouts, which is the number of lenslets (60 in short path, 46 in long path) times the number of frames (300). While the data could be improved by running several more iterations and averaging the results, the overall trends in the dropouts followed expected patterns. No dropouts were detected with atmosphere applied on SLM 2 in either the short or long path. While the WFS images showed fluctuation in the long path SLM 2 case even without atmosphere, these fluctuations are expected to increase variation in the error data if not to induce actual dropouts in the SLM 2 long path case. As expected, the error from applying atmosphere upstream at SLM 1 increases somewhat in the short path and dramatically in the long path compared to atmosphere applied in the pupil plane at SLM 2. Dropouts due to atmosphere on SLM 1 and on both SLMs represent about 0.5–1% in the short path and 5–10% in the long path.

Table 1. Intensity Dropouts in Short and Long Paths

		Short Path		Long Path	
		# Dropouts	% (of 18000)	# Dropouts	% (of 13800)
SLM 2	1 Hz	0	0	0	0
	3 Hz	0	0	0	0
	5 Hz	0	0	0	0
	7.5 Hz	0	0	0	0
SLM 1	1 Hz	208	1.16	804	5.83
	3 Hz	20	0.11	761	5.51
	5 Hz	27	0.15	1480	10.7
	7.5 Hz	15	0.08	1238	8.97
Both	1 Hz	317	1.76	865	6.27
	3 Hz	97	0.54	758	5.49
	5 Hz	42	0.23	1498	10.9
	7.5 Hz	299	1.66	1244	9.01

Figure 9 shows the disturbance profiles on SLM 2 in the short path, while Figure 10 shows them in the long path. The different profiles represent the different rates at which atmosphere was applied on the SLMs. No control was applied, so error minimization is not expected. This data is shown to compare disturbance profile trends only. The error profiles between SLM 2 in the short path and SLM 2 in the long path are comparable as expected, with slightly more variation in the long path disturbance data, as well as more noise on the disturbance profiles. Some differences in the timing or the amount of atmospheric realization that passes in the same 20 seconds of data collection in various cases are due to imperfect timing control using Simulink's hardware interface.

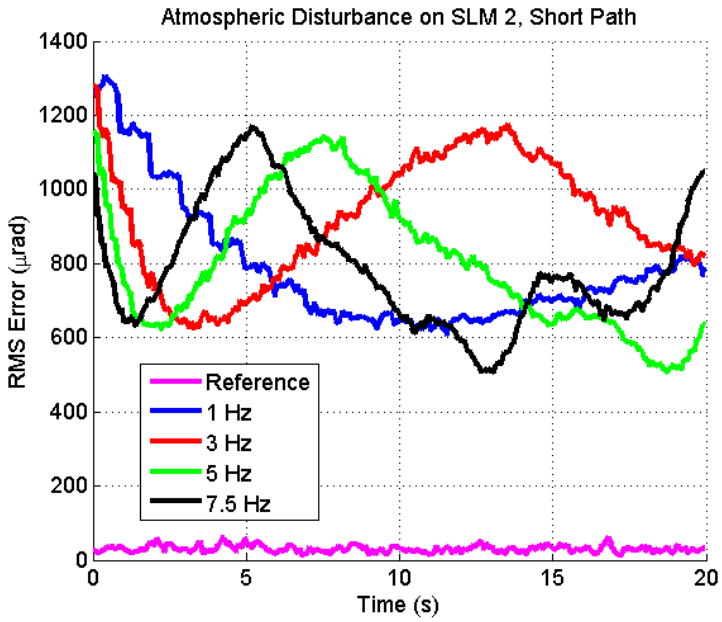

Figure 9 – Atmospheric disturbance at different rates on SLM2 in short path

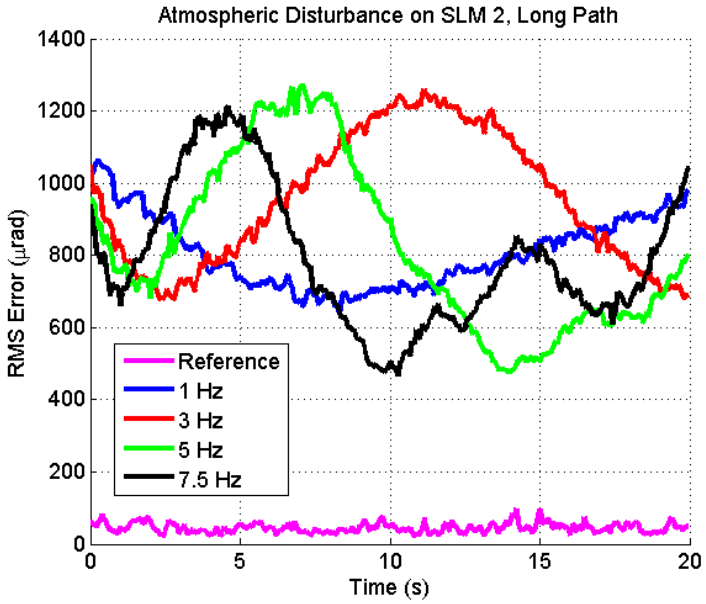

Figure 10 – Atmospheric disturbance at different rates on SLM2 in long path

3.3 Scintillation analysis approximation

From the wavefront sensor data the amount of scintillation, or the scintillation index, σ_I^2, can be obtained by using the relation:

$$\sigma_I^2 = \frac{< I^2 >}{< I >^2} - 1 \qquad (1)$$

where I is the intensity and <…> is an ensemble average. From each spot in the Shack Hartmann wafefront sensor, a software mask was created and the scintillation index was calculated per mask. The average of the scintillation of all the masks per frame was taken and the procedure repeated for all recorded frames.

From σ_I^2, assuming a weak irradiance regime (σ_I^2 <1) for the long propagation path in the laboratory, the turbulence strength parameter, or the index of refraction structure parameter, C_n^2, was calculated using the Rytov variance given by

$$\sigma_{Rytov} = 1.23 C_n^2 k^{\frac{7}{6}} L^{\frac{11}{6}} \qquad (2)$$

where k is the optical wavenumber and L is the propagation distance.

Following the procedure described above from the data sets recorded for the short and long path, the scintillation index was calculated using Rytov variance. The structure constant, C_n^2, was then calculated to be 9.99x10^{-11} m$^{-2/3}$ for the short path and 4.26x10^{-11} m$^{-2/3}$ for the long path. Figures 9 and 10 show the plots of the smoothed data for the short and long paths, respectively.

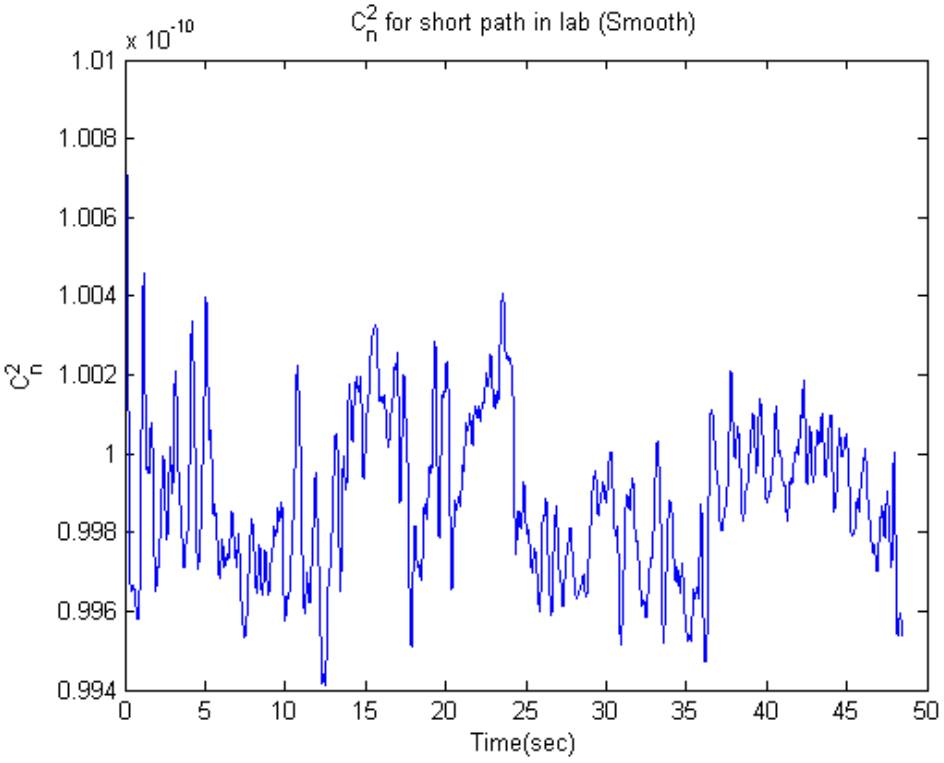

Figure 11 – Smoothed C_n^2 data in short path

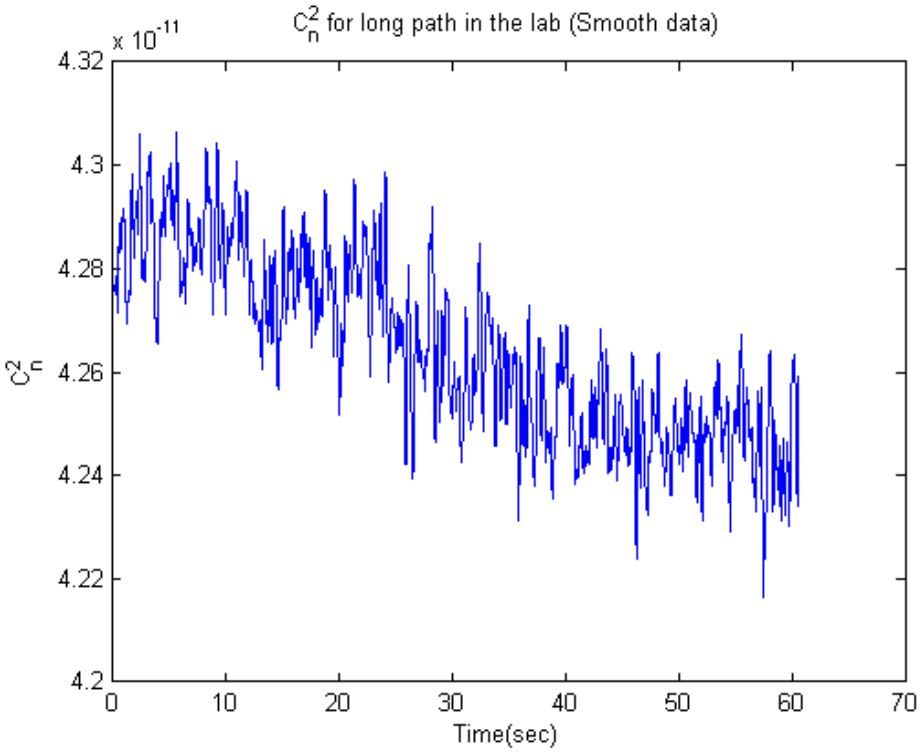

Figure 12 – Smoothed C_n^2 data in long path

The test bed must be calibrated in order to quantify the irradiance regimes for the long and short paths. Once the scintillation index for both paths is calculated as a statistical ensemble of data, the spatial light modulators will be used to introduce known atmospheric turbulence conditions. Then, the dropout detection will be implemented and compared with results from Table 1.

7.0 Conclusion

Through this work, a testbed has been developed which can be used to get a first order approximation for deep turbulence conditions. The effects of deep turbulence existing in a maritime environment were generated in the testbed by extending the beam path between the spatial light modulator phase screens where atmospheric turbulence profiles were applied. This provided a foundation for the first critical elements of a maritime environment to be simulated.

The setup allows for both short and long path configurations, single or multiple spatial light modulators for atmospheric turbulence model testing, and an adaptive optics system for testing advanced control algorithms, scintillation, and intensity dropout generation capabilities. Intensity dropouts were accounted for by assigning missing centroids to an artificial subaperture corner location. From the dropout detection tool, a quantitative comparison using Rytov variance was made between the scintillation indices in the short and long paths. In the future, additional data will be collected using the current atmospheric turbulence model in order to calibrate the test bed. This will allow more extensive beam control algorithm testing to be performed and reported.

8.0 Future Work

To produce more realistic atmospheric turbulence in the lab, SLMs with faster update rates can be investigated. SLMs running at 100 Hz or more are desirable. A fast enough WFS camera would become critical in this case.

To investigate beam control performance in the deep turbulence scenario, a method of tracking centroid trajectories or extrapolating likely positions in the case of dropouts should be developed. This will provide more accurate deep turbulence atmospheric profiles for more realistic control. Furthermore, investigation of the limits of aberrator plane separation for sufficient beam control should be performed.

With the many data collection efforts underway to improve statistical knowledge of turbulence in a maritime environment, new models will be developed to describe maritime turbulence. These models should be implemented on the current SLMs or future faster SLMs to combine near-surface effects with deep turbulence effects for a complete laboratory simulation of the maritime environment.

In additional future work, the current adaptive optics testbed will be integrated with the Naval Postgraduate School's High Energy Laser jitter control testbed. The optics table containing both systems will be configured as a ship motion simulator. In this way, a comprehensive laboratory system will be available for testing beam control algorithms in a maritime environment.

References

Fried, D. L. (1998). Branch point problem in adaptive optics. J. Opt. Soc. Am., 15 (10).

Fried, D. L., & Vaughn, J. L. (1992). Branch cuts in the phase function. J. Opt. Soc. Am., 31(15).

Hammel, S. (2007). Turbulence effects on laser propagation in a marine environment. SPIE Atmospheric Optics: Models, Measurements, and Target-In-The-Loop Propagation, 6708.

Roggemann, M. C., & Welsh, B. (1996). Imaging through turbulence. Boca Raton: CRC Press, Inc.

Sanchez, D. J., & Oesch, D. W. (2009). The aggragate behavior of branch points I – the creation and evolution of branch points. Albuquerque: Air Force Research Laboratory Technichal Paper 1012.

Santiago, F., et al. (2005). Low altitude horizontal scintillation measurements of atmospheric turbulence over the sea: experimental results. SPIE Active and Passive Optical Components for WDM Communications V, 6014, 2005.

Vetelino, F. S., et al. (2006). Initial measurements of atmospheric parameters in a marine environment. SPIE Atmospheric Propagation III, 6215.